

## A NEW PARTICLE-LIKE METHOD FOR SUPERSONIC COMBUSTION FLOW SIMULATIONS

Fábio Rodrigues Guzzo, [fabioguzzo@uol.com.br](mailto:fabioguzzo@uol.com.br)

CTA/ITA – Instituto Tecnológico de Aeronáutica

João Luiz F. Azevedo, [azevedo@iae.cta.br](mailto:azevedo@iae.cta.br)

CTA/IAE – Instituto de Aeronáutica e Espaço

**Abstract.** *The present work is concerned with hypersonic blunt body flow numerical simulations with chemical non-equilibrium. New theoretical and numerical formulations for coupling the chemical reaction to the fluid dynamics are presented and validated. The fluid dynamics is defined for a stationary unstructured mesh and the chemical reaction process is defined for “finite quantities” moving through the stationary mesh. The fluid dynamics is modeled by the Euler equations and the chemical reaction speeds by the Arrhenius law. Ideal gases are considered. The thermodynamical data are based on JANNAF tables and Burcat’s database. The algorithm proposed by Liou, known as AUSM+, is implemented in a cell-centered based finite volume method and in an unstructured mesh context. Multidimensional limited MUSCL interpolation method is used to perform property reconstructions and to achieve second-order accuracy in space. The minmod limiter is used. The second order accuracy, five stage, Runge-Kutta time-stepping scheme is employed to perform the time march for the fluid dynamics. The numerical code VODE, which is part of the CHEMKIN-II package, is adopted to perform the time integration for the chemical reaction equations. The freestream reacting fluid is composed of H<sub>2</sub> and air at the stoichiometric ratio. The emphasis of the present paper is on the description of the new methodology for handling the coupling of chemical and fluid mechanic processes. The results included in the paper have the objective of validating the proposed methodology. The configuration considered is a hypersonic flow over a blunt body. The detonation wave is induced by the shock wave. Solutions obtained for two meshes are shown, compared and analyzed. The numerical solutions are also compared with experimental data.*

**Keywords:** *hypersonic flows, numerical simulations, chemical non-equilibrium, CFD.*

### 1. INTRODUCTION

This work is part of a continuing effort that is being carried out in CTA/IAE (Comando-Geral de Tecnologia Aeroespacial / Instituto de Aeronáutica e Espaço) to develop numerical methods to simulate dynamic fluids. The objective of this effort is to conceive comprehensive codes and to test and validate them over simple configurations in which experimental, analytical or numerical solutions are available in the literature. The present paper addresses specifically hypersonic flow problems in which chemical non-equilibrium is present. Hence, there are effects arising from the chemical non-equilibrium condition that cannot be neglected.

Hypersonic flow problems including chemical reactions have become important since the end of the World War II with the advent of rockets, hypersonic aircrafts and atmospheric reentry vehicles. For reentry vehicles, the gas dynamic problems become all the more challenging since the flight trajectories traverse a wide range of Mach, Knudsen, Reynolds and Damköhler numbers (Sarma, 2000). The full range of molecular physical phenomena of reentry flights encompasses rarefaction, ionization, radiation, relaxation and thermal and compositional nonequilibrium (Sarma, 2000). For hypersonic aircrafts, the combustion in the engine may take place at supersonic speeds, as in Scramjets (Supersonic Combustion Ramjets) and Shramjets (Shock-Induced Combustion Ramjets) (Ahuja *et al.*, 1992). CTA/IAE is developing a recoverable orbital platform for experimentation in microgravity environment, called SARA (Satélite de Reentrada Atmosférica).

Development of a solver for reactive hypersonic flow applications started in CTA/IAE at the end of 1990s. Successful validations of the numerical formulations and the physico-chemical data were carried out over simulations for reactive flows composed of a stoichiometric H<sub>2</sub>-Air mixture (Azevedo and Figueira da Silva, 1997, Korzenowski, 1998, Figueira da Silva *et al.*, 1999, Pimentel, 1999, Figueira da Silva *et al.*, 2000). Hypersonic flows around wedges were considered. In these configurations, the oblique shock wave triggers the combustion that eventually takes the form of an oblique detonation wave. Comparisons between numerical and experimental results showed a good agreement concerning the overall structure of the flow. Nevertheless, the first trial to simulate a reactive flow composed of the same mixture around a blunt projectile had not been successful (Guzzo, 2003). The configuration simulated was Lehr’s experiment with a steady flow around a sphere-cylinder (Lehr, 1972). The experiment shadowgraph showed that normal shock and the reaction front near the stagnation line seem coupled. These two fronts distance from each other downstream and the detachment reveals noticeable as the shock wave becomes more oblique. The first simulation obtained was considered unsuccessful since the detachment had not been observed in the numerical solution (Guzzo, 2003). The reaction front remained visibly coupled to the shock wave for the overall solution. The differences between the numerical simulations and the experimental data can be attributed either to numerical errors or to improperly

modeled chemical kinetics. The physics of these flows are predominantly driven by reaction kinetics and convection phenomena (Wilson and MacCormack, 1990). The uncertainties of diffusion and mixing can be neglected.

Several authors investigated and simulated both Lehr's steady and unsteady cases (Lee and Deiwert, 1989, Yungster *et al.*, 1989, Wilson and MacCormack, 1990, Matsuo and Fujiwara, 1991, Sussman and Wilson, 1991, Ahuja *et al.*, 1992, Singh *et al.*, 1992, Ess and Allen, 2005). Lee and Deiwert (1989) and Yungster *et al.* (1989) simulated Lehr's experimental data for Mach 4.18, 5.11 and 6.46. They used Euler equations and a 6-species plus an inert gas such as Argon or Nitrogen and 8-reactions chemistry model. The flow field for Mach 4.18 and 5.11 was found to be steady in contrast to the experimental evidence that the flow field is, indeed, unsteady. The grids used were not sufficient to resolve the flow field correctly (Ahuja *et al.*, 1992). Wilson and MacCormack (1990) used Euler equations and a 13-species and 33-reactions chemistry model. They showed the validity of the reaction model and the importance of grid resolution needed to properly model the flow physics. The calculations were not time accurate, so the unsteady behavior was not captured (Ahuja *et al.*, 1992). Sussman and Wilson (1991) also used Euler equations and a 13-species and 33-reactions chemistry model to simulate the flow field for Mach number of 4.79. They have proposed a new formulation based on logarithmic transformation. It greatly reduces the number of grid points needed to properly resolve the induction zone. They successfully simulated the unsteady case (Ahuja *et al.*, 1992). However, frequency was slightly underpredicted. Ahuja *et al.* (1992) used Navier-Stokes equations and a 7-species and 7-reactions chemistry model to simulate the flow field for Mach 5.11 and 6.46. They successfully simulated the unsteady case and the frequency oscillation was found to be in a good agreement with the experimentally observed frequency (Ahuja *et al.*, 1992). Matsuo *et al.* (1995) used Euler equations and a 8-species and 19-reactions chemistry model to simulate the flow field for Mach 4.18 and 4.79. A fine grid distribution, such as 161 x 321, was used and they have obtained successful solutions with a good agreement concerning the frequency of the oscillations.

There is a major difference between simulating the steady and the unsteady cases. For the flow field with an unstable reaction front, the critical zone that requires accurate solution is the region near the stagnation line, between the normal shock wave and projectile leading edge. The unsteady pattern of the overall flow field is due to the convection triggered by the coupled oscillatory reaction front and the convective phenomena in this region of the flow. In the other hand, for the steady case, the numerical solution must be accurate in the region of the induction zone just before the oblique reaction front. In this region, as the shock wave becomes more oblique and the temperature increment diminishes, the detonation wave gradually aligns to the local flow. As long as the chemical kinetics is strongly non-linear with the species mass fraction, the simulation must be able to properly simulate the induction zone in a region of flow that progressively tightens to reacted gases. Ahuja and Tiwari (1994) used Navier-Stokes equations and a 9-species and 18-reactions chemistry model to simulate Lehr's experiment for Mach 6.46, which is a steady flow. The detachment between the shock wave and the reaction front was not clearly noticeable. Ess and Allen (2005) simulated Lehr's experiments for Mach 4.48 and 6.46. They used Navier-Stokes equations and a 9-species and 19-reactions chemistry model. They successfully simulated the unsteady flow field for Mach 4.48 and the oscillation frequency compares well with the frequency obtained experimentally (Ess and Allen, 2005). In the steady flow for Mach 6.46, they used two mesh in order to demonstrate the sensitivity of the physical problem to spatial resolution. In the coarse mesh, with half the cell number in both directions, the shock and the reaction fronts remained visually attached. In the finer mesh, the detachment is barely observable. Wilson and Sussman (1993) simulated Lehr's experiment for Mach 6.46. They obtained a good agreement with the experiment concerning the position of the shock wave and the reaction front. They used a coarse mesh, such as 52 x 52 grid. Probably, the format of the mesh may have contributed to reduce the numerical diffusion of the species mass fractions. In the oblique detonation wave region, the diffusion of the mass fraction is minimized if the faces of the cells that separate unreacted gases to reacted gases are align to the local flow. The mesh influence in the solution may have been significant in the success of the simulation. Wilson and MacCormack (1992) also successfully simulated Lehr's experiment for Mach 6.46 using an adaptative mesh algorithm. The final mesh format probably contributed in the reduction of the numerical diffusion and in the success of the simulation as well.

With the objective of better simulating the flowfield in the region near the oblique detonation wave that progressively aligns to the local flow, a new formulation is proposed in the present paper to couple the chemical kinetics to the fluid dynamics. It is a simple Eulerian/Lagrangian hybrid methodology. The fluid dynamics is defined for a stationary unstructured mesh and the chemical kinetics is defined for finite quantities, or particles, moving through the stationary mesh. The objective for adopting Lagrangian particles is to avoid that the chemical reaction process considers average species mass fractions. The particles carry the chemical composition information and the reaction is performed over each particle independently. The interface Eulerian/Lagrangian is conducted in a such way that the density, speed and the internal energy values of the particles are defined as being equal to the values of the control volume that contains the particle, whereas the mass fraction of the control volume is defined as being equal to the weight averaged mass fractions of the chemical composition of the particles contained in the volume.

Simulations of Lehr's experiment for Mach 6.46 performed over two different meshes are here presented. Analyses of the solutions obtained and comparisons between the solutions and with the experimental data are shown. Although the formulation is for unstructured grids, only structured meshes were employed. Guzzo and Azevedo (2006) have

shown that the regularity and the smoothness of the computational meshes have had a very positive effect on the quality of solutions.

## 2. NUMERICAL FORMULATION

An Eulerian/Lagrangian hybrid methodology is employed. The fluid dynamics is defined for a stationary mesh and the chemical kinetics is performed for particles that move through the stationary mesh.

### 2.1. Eulerian Method

The fluid dynamics is modeled by the axisymmetric Euler equations applied over stationary meshes. Four equations are included; the continuity, two component momentum and the energy equations. The species equations are not considered. The integral form of the Euler equations were written for the  $i$ -th volume as

$$V_i \frac{\partial}{\partial t} (\mathbf{Q}_i) + \oint_{S_i} (\mathbf{E}rdr + \mathbf{F}dz) + \mathbf{H}_i V_i = 0, \quad (1)$$

where  $r$  is the radial coordinate,  $z$  is the axial coordinate and  $V_i$  is the volume of the  $i$ -th cell.  $\mathbf{Q}$  is the vector of the conserved variables,  $\mathbf{E}$  and  $\mathbf{F}$  are the inviscid flux vector and  $\mathbf{H}$  is the axisymmetric source term. The definition of these terms is

$$\mathbf{Q} = \begin{bmatrix} \rho \\ \rho u_z \\ \rho u_r \\ \rho \mathcal{E} \end{bmatrix}, \quad \mathbf{E} = \begin{bmatrix} \rho u_z \\ \rho u_z^2 + p \\ \rho u_z u_r \\ u_z (\rho \mathcal{E} + p) \end{bmatrix}, \quad \mathbf{F} = \begin{bmatrix} \rho u_r \\ \rho u_z u_r \\ \rho u_r^2 + p \\ u_r (\rho \mathcal{E} + p) \end{bmatrix}, \quad \mathbf{H} = \begin{bmatrix} 0 \\ 0 \\ -p/r \\ 0 \end{bmatrix}. \quad (2)$$

In this expression,  $\rho$  is the density,  $u_r$  and  $u_z$  are the velocity components in the radial and axial coordinates,  $\mathcal{E}$  is the total energy and  $p$  is the pressure.

Liou's upwind, flux vector splitting method (Liou, 1994, Liou, 1996), known as AUSM+, is implemented in a cell centered-based, finite volume code for unstructured meshes. The reinterpretation of the formulation for unstructured meshes follows Azevedo and Korzenowski (1998). The 2nd-order spatial accuracy is obtained using the MUSCL reconstruction (van Leer, 1979) and the MINMOD limiter (Hirsch, 1988) to extrapolate the primitive variables from the centroid to the faces of the cells. The second-order accuracy, five-stage Runge-Kutta (Mavriplis, 1988, Mavriplis, 1990) scheme is employed to perform the time march. The boundary conditions were implemented with the use of "ghost", or "slave", cells. For solid wall boundary, the velocity component normal to the wall in the ghost volume has the same magnitude and opposite sign of this variable in its adjacent interior volume, whereas the velocity component tangent to the wall is equal to its internal cell counterpart. For the other properties, zero normal gradients are assumed at the wall. For the entrance boundary, the flow variables receive the freestream values. For the subsonic exit boundary, three properties are extrapolated from interior information. For a supersonic exit boundary, all properties are extrapolated from interior information. For the initial condition, freestream conditions are specified throughout the flowfield. Further details on the boundary and initial conditions are described by Guzzo (2006).

### 2.2. Lagrangian Method

The chemical kinetics is defined for particles that move with the fluid. The chemical composition of the  $p$ -th particle is defined as

$$\frac{DY_p}{Dt} = \dot{\Omega}_p, \quad (3)$$

where  $\mathbf{Y}$  is the vector of the chemical species mass fractions and  $\dot{\Omega}$  is the chemical source vector, which are written as

$$\mathbf{Y} = \begin{bmatrix} \rho Y_1 \\ \rho Y_2 \\ | \\ \rho Y_M \end{bmatrix}, \quad \dot{\Omega} = \begin{bmatrix} \dot{w}_1 \\ \dot{w}_2 \\ | \\ \dot{w}_M \end{bmatrix}. \quad (4)$$

$Y_k$  is the mass fraction and  $\dot{w}_k$  is the mass production term of the  $k$ -th chemical species. The chemical reaction kinetics is modeled by the Arrhenius law. The VODE numerical code (Byrne and Dean, 1993) is adopted to perform the time integration for the chemical reactions. The reaction rate for each species is determined with the use of the CHEMKIN-II code (Kee *et al.*, 1991). The variation of the particle position is defined as

$$\frac{Dr_p}{Dt} = (u_r)_p, \quad \frac{Dz_p}{Dt} = (u_z)_p. \quad (5)$$

A simple first-order accuracy, one-stage method is employed to update the position of the particles from the stage  $n$  to the stage  $n+1$ ,

$$\begin{aligned} z_{ji}^{n+1} &= z_{ji}^n + (u_z)_i^n \cdot \Delta t^n, \\ r_{ji}^{n+1} &= r_{ji}^n + (u_r)_i^n \cdot \Delta t^n. \end{aligned} \quad (6)$$

For the initial condition, one particle was added in each cell and a weight,  $wp$ , is attributed to it, defined as

$$wp_p = r_i \cdot [\max(r_{il}) - \min(r_{il})], \quad l = 1, 2, \dots, (N_n)_i, \quad (7)$$

where,  $r_i$  is radial coordinate of the  $i$ -th cell's center,  $r_{il}$  is the radial coordinate of its  $l$ -th node and  $(N_n)_i$  is its number of nodes. For the entrance boundary, one particle is created periodically in the center of each cell that shares a face with the boundary. A fixed and a unique time value was employed for the overall boundary cells. The weight of the particles created in the entrance boundary is defined as

$$wp_p = r_i \cdot [\text{abs}(r_{i1} - r_{i2})], \quad (8)$$

where  $r_{i1}$  and  $r_{i2}$  are the radial coordinates of the two nodes of the  $i$ -th cell located in the boundary. When a particle crosses the exit boundary, this particle is neglected. When a particle crosses a solid wall or an axisymmetric boundary, this particle is reallocated inside the flow field. The particle is positioned in the boundary surface, in the nearest point of the original outside position.

### 2.3. Eulerian-Lagrangian Interface

The chemical composition of the control volume is defined as being equal to the weight averaged chemical composition of the particles contained in the volume,

$$(Y_k)_i = \frac{\sum_{j=1}^{(N_p)_i} [(Y_k)_{ji} \cdot wp_{ji}]}{\sum_{j=1}^{(N_p)_i} wp_{ji}}, \quad (9)$$

where the  $(N_p)_i$  is the number of particles contained in the  $i$ -th control volume,  $(Y_k)_{ji}$  is the mass fraction of the  $k$ -th chemical species of the  $j$ -th particle contained in the  $i$ -th volume and  $wp_{ji}$  is the weight attributed to the particle. If a control volume contains no particles, the particles contained in the neighbor cells are considered,

$$(Y_k)_i = \frac{\sum_{l=1}^{(N_v)_i} \left( \sum_{j=1}^{(N_p)_l} [(Y_k)_{jl} \cdot wp_{jl}] \right)}{\sum_{l=1}^{(N_v)_i} \left( \sum_{j=1}^{(N_p)_l} wp_{jl} \right)}, \quad (10)$$

where  $(N_v)_i$  is the number of cells that share one face with the  $i$ -th volume and  $(N_p)_l$  is the number of particles contained in the  $l$ -th neighbor. If there are no particles in the control volume and in its neighbors, the chemical

composition of the control volume is not updated. The density, speed and the internal energy of the  $j$ -th particle contained in the  $i$ -th control volume are defined as being equal to the values of the control volume,

$$\rho_{ji} = \rho_i, (u_z)_{ji} = (u_z)_i, (u_r)_{ji} = (u_r)_i, e_{ji} = e_i. \quad (11)$$

A temperature limiter was employed. In the simulations performed, when the fluid crosses the oblique detonation wave, as the mixture reacts, the chemical energy is released and the internal energy of the gas decreases due to the gas expansion. The internal energy was considered to be composed of the chemical and thermal energies. If a particle crosses the oblique reaction front without reacting, its temperature drops and it remains unreacted. The temperature limiter is a simple solution used to avoid that particles very close to each other carry very different chemical composition. The interested reader is referred to the work by Guzzo (2006) for further details on the temperature limiter. The temperature of the particle, considering the limiter was defined as

$$T_{ji} = \max(T_{ji}^{(0)}, \min(T_i, T_{il})), \quad l = 1, 2, \dots, (N_v)_i, \quad (12)$$

where  $T_{ji}^{(0)}$  is the temperature of the particle without the limiter.  $T_i$  is the temperature of the control volume that contains the particle and  $T_{il}$  is temperature of its  $l$ -th neighbor volume.

The time advancement of the solution from the  $n$ -th stage to the  $(n+1)$ -th stage is achieved by three independently steps; one step for the fluid dynamics, one step for the chemical reaction process and one step for the particle position, written as

$$\begin{aligned} \mathbf{Q}_i^{n+1} &= \mathcal{L}(\mathbf{Q}_i^n, \Delta t^n), \\ \mathbf{Y}_{ji}^{n+1} &= \mathcal{Q}(\mathbf{Y}_{ji}^n, \Delta t^n), \\ \mathbf{r}_{ji}^{n+1} &= f(\mathbf{r}_{ji}^n, \mathbf{Q}_i^n, \Delta t^n), \end{aligned} \quad (13)$$

where  $\mathcal{L}$  is the operator of the fluid dynamics,  $\mathcal{Q}$  is the chemistry operator and  $f$  is the particle position operator.  $\mathbf{r}_{ji}$  is the position vector of the particles, which is written as

$$\mathbf{r} = \begin{bmatrix} z \\ r \end{bmatrix}. \quad (14)$$

$\Delta t^n$  is the time step of the  $n$ -th stage. A time step for each cell is calculated,  $\Delta t_i^n$ , and a single value,  $\Delta t^n$ , is used.  $\Delta t^n$  is the minimum value of the  $\Delta t_i^n$ . The time step for each cell is calculated such that the CFL number is kept approximately constant throughout the field (Figueira da Silva *et al.*, 1999).

#### 2.4. Constitutive Equations

The Balakrishnan and Williams (1993) chemical kinetics mechanism is selected to model the H<sub>2</sub> and air reactive mixture. The thermodynamic properties are defined using the polynomial tables of JANNAF (Anon, 1970) and Burcat's database (Burcat, 1984).

### 3. RESULTS AND DISCUSSION

A supersonic flow composed of a stoichiometric H<sub>2</sub>-air mixture over a sphere-cylinder of 15 mm diameter was simulated. The configuration is the same of Lehr's experiment for Mach number equal to 6.46 (Lehr, 1972). The free-stream conditions are  $T_\infty = 292$  K and  $p_\infty = 320$  mmHg. Two simulations were carried out over two different structured quadrilateral meshes. The two meshes differ from each other in refinement and format. The boundaries of the meshes are presented in the Fig. 1. The coarse mesh, Grid 1, is composed of 6000 nodes and 5831 cells, in which the distribution is  $50 \times 120$  points in the normal and longitudinal directions, respectively. The fine mesh, Grid 2, is composed of 25000 nodes and 24651 cells, in which the distribution is  $100 \times 250$  points in the normal and longitudinal directions, respectively. For both meshes, the nodes are equally spaced in each direction. Position coordinates are in centimeters.

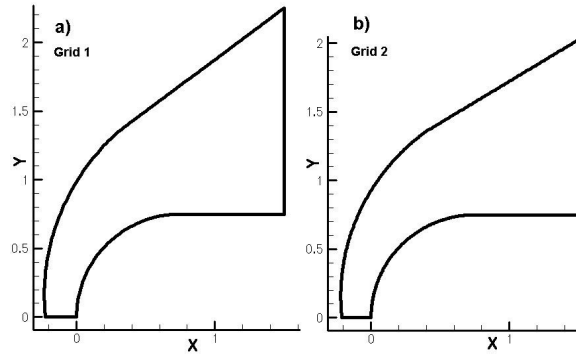


Figure 1. Borders of the meshes: a) Coarse mesh ( $50 \times 120$ ), Grid 1; b) Fine mesh ( $100 \times 250$ ), Grid 2.

Figure 2 shows the density and the  $H_2O$  mass fraction contours of the solutions obtained for the two meshes. The same pattern of Lehr's experiment (Lehr, 1972) is observed in the numerical solutions. Near the stagnation line, it is not possible to distinguish the reaction front from the normal shock wave. As the shock wave becomes more oblique downstream, the two fronts distance from each other.

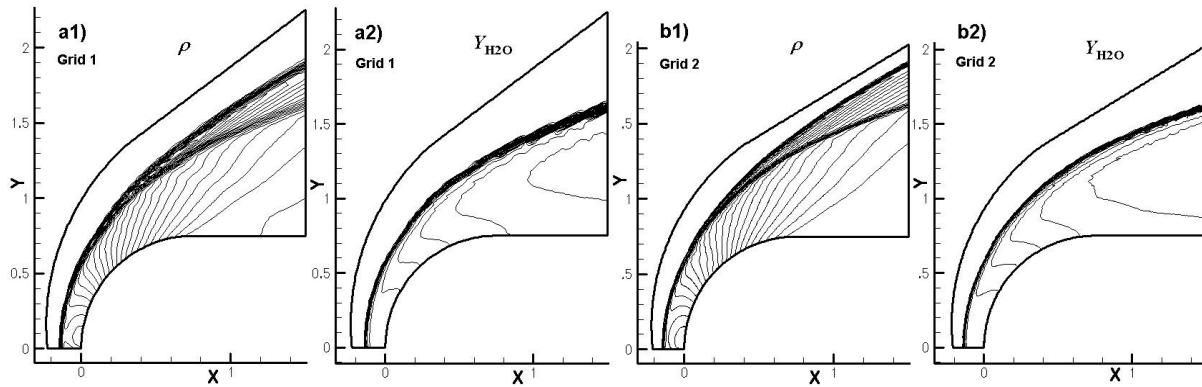


Figure 2. Density and the  $H_2O$  mass fraction contours: a1) Grid 1 density contours; a2) Grid 1  $H_2O$  mass fraction contours; b1) Grid 2 density contours; b2) Grid 2  $H_2O$  mass fraction contours.

Figure 3 shows the position of the shock wave and the reaction front for the two solutions and for the experimental data. For the numerical solutions, in order to indicate the position of the fronts in the figure, four temperature contours were included. The influence of the refinement and the format of the mesh was not significant, since the numerical solutions compare well to each other. Comparisons between the numerical solution and the experiment shadowgraph showed good agreement concerning the shock wave and the reaction front positions, although the last was slightly dislocated. Although not completely coincident with the experiment, the solutions obtained indicated that the numerical errors may have been reduced with the use of the current formulation. Differences between numerical simulations and experimental data can be attributed either to numerical errors or to improperly modeled chemical kinetics.

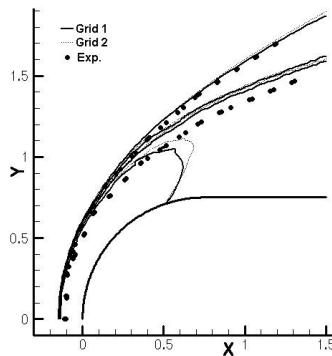


Figure 3. Position of the shock wave and reaction front. Comparison to experimental data (Lehr 1972).

Figure 4 shows zooms of two regions of the flow solution over Grid 2, near the normal and near the oblique reaction fronts. This visualization evidences the challenges of the simulation. Within the same flow field, the regime goes from frozen (Damköhler number  $\ll 1$ ) to equilibrium (Damköhler number  $\gg 1$ ). The Damköhler number is defined as the flow timescale over the chemical reaction timescale, and is used to relate chemical reaction timescale to other phenomena occurring in a system. Figure 4 a) shows that the chemical reaction timescale is much lower than the convective time scale, the gas reacts nearly instantaneously, whereas Fig. 4 b) shows the opposite behavior away from the stagnation region. The streamtraces show how the reaction front aligns to the local flow as the shock and reaction fronts become more oblique. As long as the chemical kinetics is strongly non-linear with the chemical composition, the use of average species mass fraction over an arbitrary mesh format to simulate this region of the flow may require a prohibitive grid refinement.

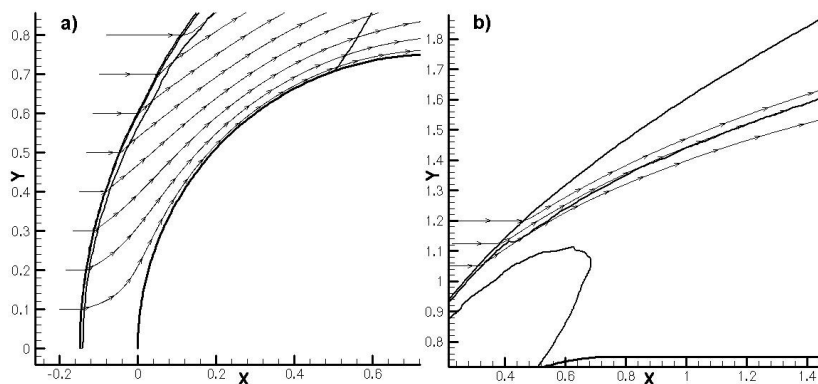


Figure 4. Zoom over Grid 2 solution with streamtraces: a) Normal reaction front; b) Oblique reaction front.

#### 4. CONCLUDING REMARKS

A simple Eulerian/Lagrangian hybrid methodology was proposed and its formulation presented. The objective for adopting Lagrangian particles was to avoid that the chemical reaction process considers average species mass fractions. Lehr's experiment for Mach number equal to 6.46 (Lehr, 1972) was successfully simulated for two meshes. The grids differ in refinement and format. Both solutions compare well to each other, indicating that the numerical errors may have been reduced with the use of the current formulation. The overall structure of the flow showed a good agreement with the experimental data. The shock wave position showed a good agreement, and the reaction front presented the same incline but a slight dislocation from the experiment position.

#### 5. ACKNOWLEDGEMENTS

The authors gratefully acknowledge the partial support for this research provided by Conselho Nacional de Desenvolvimento Científico e Tecnológico, CNPq, under the Integrated Project Research Grants No. 501200/2003-7 and 312064/2006-3.

#### 6. REFERENCES

- Ahuja, J.K., Tiwari, S.N., and Singh, D.J., 1992, "Investigation of Hypersonic Shock-Induced Combustion in a Hydrogen-Air System," 30th AIAA Aerospace Sciences Meeting and Exhibit, AIAA Paper No. 1992-0339, Reno, NV.
- Ahuja, J.K., and Tiwari, S.N., 1994, "A Parametric Study of Shock-Induced Combustion in a Hydrogen-Air System," 32nd Aerospace Science Meeting and Exhibit, AIAA Paper No. 1994-674, Reno, NV.
- Anon, 1970, "JANNAF: Thermochemical Tables," Dow Chemical Co. Midland, Mich.
- Azevedo, J.L.F., and Figueira da Silva, L.F., 1997, "The Development of an Unstructured Grid Solver for Reactive Compressible Flow Applications," Proceedings of the 33rd AIAA/ASME/SAE/ASEE Joint Propulsion Conference & Exhibit, Seattle, WA, Estados Unidos.
- Azevedo, J.L.F., e Korzenowski, H., 1998, "Comparison of Unstructured Grid Finite Volume Methods for Cold Gas Hypersonic Flow Simulations", AIAA Paper No. 98-2629, Proceedings of the 16th AIAA Applied Aerodynamics Conference, Albuquerque, NM, pp. 447-463.
- Balakrishnan, G., e Williams, F.A., 1993, "Turbulent Combustion Regimes for Hypersonic Propulsion Employing Hydrogen-Air Diffusion Flames," Journal of Propulsion and Power, Vol.10, No 3, pp.434-436.
- Burcat, A., 1984, "Thermochemical Data for Combustion Calculations," Combustion Chemistry, W.C. Gardiner, Ed, Springer-Verlag, New York.

- Byrne, G.D., and Dean, A.M., 1993, "The Numerical Solution of Some Kinetics Models with VODE and CHEMKIN II," *Computers Chem.*, Vol. 17, No. 3, pp. 297-302.
- Ess, P.R., and Allen C.B., 2005, "Parallel Computation of Two-Dimensional Laminar Inert and Chemically Reactive Multi-Species Gas Flows," *International Journal for Numerical Methods in Heat & Fluid Flow*, Vol. 15, No 3, pp. 228 – 256.
- Figueira da Silva, L.F., Azevedo, J.L.F., e Korzenowsk, H., 1999, "On the Development of an Unstructured Grid Solver for Inert and Reactive High Speed Flow Simulations", *Journal of the Brazilian Society of Mechanical Sciences*, Vol. 21, No. 4, pp. 564-579.
- Figueira da Silva, L.F., Azevedo, J.L.F., and Korzenowski, H., 2000, "Unstructured Adaptive Grid Flow Simulations of Inert and Reactive Gas Mixture," *Journal of Computational Physics*, Vol. 160, No. 2, pp. 522-540.
- Guzzo, F.R., 2003, "Análise e Simulação de Escoamentos Hipersônicos em Condição de Não Equilíbrio Químico," *Trabalho de Graduação, ITA, São José dos Campos, SP, Brasil.*
- Guzzo, F.R. and Azevedo, J.L.F., 2006, "Mesh Topology Influence on Supersonic Blunt Body Flow Simulations," *Proceedings of the 11th Brazilian Congress of Thermal Sciences and Engineering, Paper CIT06-0474, Curitiba, Brazil.*
- Guzzo, F.R., 2006, "Análise e Simulação da Combustão Induzida por Projéteis em Velocidades Hipersônicas," *Tese de Mestrado, ITA, São José dos Campos, SP, Brasil.*
- Hirsch, C., 1988, *Numerical Computational of Internal and External Flows*, Vols. 2, Wiley, New York.
- Kee, R.J., Rupley, F.M., and Miller, J.A., 1991, "CHEMKIN-II: A Fortran Chemical Kinetics Package for the Analysis of Gas Phase Chemical Kinetics," *Sandia National Laboratories, Technical Rep. SAND86-8009B/UC-706.*
- Korzenowski, H., 1998, "Técnicas em Malhas Não Estruturadas para Simulação de Escoamentos a Altos Números de Mach," *Tese de Doutorado, ITA, São José dos Campos, SP.*
- Lee, S., and Deiwert, G.S., 1989, "Calculation of Nonequilibrium Hydrogen-Air Reactions with Implicit Flux Vector Splitting Method," *24th Thermophysics Conference, AIAA Paper No. 89-1700, Buffalo, NY.*
- Lehr, H.F., 1972, "Experiments on Shock-Induced Combustion," *Astronautica Acta*, Vol 17, No. 4 & 5, pp. 589 - 597.
- Liou, M.S., 1994, "A Continuing Search for a Near-Perfect Numerical Flux Scheme. Part I: AUSM+," *NASA TM-106524, NASA Lewis Research Center, Cleveland, OH.*
- Liou, M.S., 1996, "A Sequel to AUSM: AUSM+," *Journal of Computation Physics*, Vol. 129, No. 2, pp. 364-382.
- Matsuo, A., and Fujiwara, T., 1991, "Numerical Simulation of Shock-Induced Combustion around an Axisymmetric Blunt Body," *26th Thermophysics Conference, AIAA Paper No. 91-1414, Honolulu, HI.*
- Matsuo, A., Fujii, K. and Fujiwara, T., 1995, "Flow Features of Shock-Induced Combustion Around Projectile Traveling at Hypervelocities," *AIAA Journal*, Vol. 33, No. 6, pp. 1056-1063.
- Mavriplis, D.J., 1988, "Multigrid Solution of the Two-Dimensional Euler Equations on Unstructured Triangular Meshes," *AIAA Journal*, Vol. 26, No. 7, pp. 824-831.
- Mavriplis, D.J., 1990, "Accurate Multigrid Solution of the Euler Equations on Unstructured and Adaptive Meshes," *AIAA Journal*, Vol. 28, No. 2, pp. 213-221.
- Pimentel, C.A.R., 2000, "Estudo Numérico da Transição entre uma Onda de Choque Oblíqua Estabilizada por um Diedro e uma Onda de Detonação Oblíqua," *Tese de Doutorado, ITA, São José dos Campos, SP.*
- Sarma, G.S.R., 2000, "Physico-Chemical Modelling in Hypersonic Flow Simulation," *Progress in Aerospace Science*, Vol. 36, No. 3, pp. 281-349.
- Singh, D.J., Ahuja, J.K., and Carpenter M.H., 1992, "Numerical Simulation of Shock-Induced Combustion/Detonation," *Symposium on High-Performance Computing for Flight Vehicles, Washington, D.C..*
- Sussman, A.M., and Wilson, G.J., 1991, "Computation of Chemically Reacting Flow Using a Logarithmic Form of the Species Conservation Equations," *Proceedings of the 4th International Conference on Numerical Combustion, Tampa, FL, pp. 224-227.*
- van Leer, B., 1979, "Towards the Ultimate Conservative Difference Scheme. V. A Second-Order Sequel to Godunov's Method," *Journal of Computational Physics*, Vol. 32, No. 1, pp. 101-136.
- Wilson, G.J., and MacCormack, R.W., 1990, "Modeling Supersonic Combustion Using a Fully-Implicit Numerical Method," *26th AIAA/ASME/SAE/ASEE Joint Propulsion Conference, AIAA Paper No. 90-2307, Orlando, FL.*
- Wilson, G.J., and MacCormack, R.W., 1992, "Modeling Supersonic Combustion Using a Fully-Implicit Numerical Method," *AIAA Journal*, Vol. 30, No. 4, pp. 1008-1015.
- Wilson, G.J., and Sussman, M.A., 1993, "Computation of Unsteady Shock-Induced Combustion Using Logarithmic Species Conservation Equations," *AIAA Journal*, Vol. 31, No. 2, pp. 294-301.
- Yungster, S., Eberhardt, S., and Bruckner, A.P., 1989, "Numerical Simulation of Shock-Induced Combustion Generated by High-Speed Projectiles in Detonable Gas Mixtures," *27th Aerospace Sciences Meeting, AIAA Paper No. 89-0673, Reno, NV.*

## 7. RESPONSIBILITY NOTICE

The authors are the only responsible for the printed material included in this paper.